JACS
JOURNAL OF THE AMERICAN CHEMICAL SOCIETY
Communication
pubs.acs.org/JACS

High-Spin Organic Diradical with Robust Stability

Nolan M. Gallagher,[†] Jackson J. Bauer,[†] Maren Pink,[‡] Suchada Rajca,[†] and Andrzej Rajca*[,†]

[†]Department of Chemistry, University of Nebraska—Lincoln, Lincoln, Nebraska 68588-0304, United States
[‡]IUMSC, Department of Chemistry, Indiana University, Bloomington, Indiana 47405-7102, United States

Supporting Information

ABSTRACT: Triplet ground-state organic molecules are interesting with respect to several emerging technologies but typically exhibit limited stability. We report two organic diradicals, one of which possesses a triplet ground state ($2J/k_B$ = 234 ± 36 K) and robust stability at elevated temperatures. We are able to sublime this high-spin diradical under high vacuum at 140 °C with no significant decomposition.

Organic molecules with high-spin ground states possess inherently fascinating electronic structures. Their characteristic spin alignment contradicts the overwhelming tendency toward spin-pairing in molecular systems, exemplified by chemical bonding.[1−3] Such molecules are attractive candidates as building blocks for magnetic materials[4−7] and in the development of spintronics.[8] For instance, open-shell molecules have been predicted to possess interesting spin transport properties, and various organic spin filters utilizing organic diradicals have been proposed.[9−13]

High-spin molecules that possess both strong ferromagnetic interactions between unpaired electrons and robust thermal stability could enable experimental verification of these novel properties predicted with theory. However, only a limited number of high-spin diradicals possess both stability permitting isolation and a singlet−triplet energy gap (ΔE_{ST}) on the order of RT (thermal energy at room temperature ~0.6 kcal mol^{-1}).[14−22] Furthermore, little is known about their stability at higher temperatures and in the vapor phase, a necessary consideration for growing organic films using chemical vapor deposition-based techniques.[23,24] Robust stability, spanning a wide temperature range, and in particular, permitting sublimation, would facilitate material processing and device fabrication. To the best of our knowledge, only two isolable high-spin diradicals, nitroxide-substituted nitronyl nitroxide (NSNN) and iminonitroxide (NSIN), undergo sublimation at 55−70 °C, facilitated by their low molecular weights.[15] The major drawback of these molecules is the lack of flexibility in the molecular design associated with their compact structures.

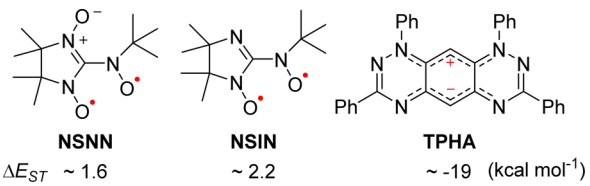

In the search for high-spin organic molecules with robust stability, we were drawn to the 1,2,4-benzotriazinyl (Blatter) radical, a thermally robust monoradical.[25] Recently, we have shown that the unique stability of a Blatter monoradical derivative permits vapor-based fabrication of thin films that exhibit excellent air/vacuum stability and retention of the paramagnetic character in thin films for at least several months.[24] We note that the Blatter radical has not been utilized as a high-spin building block. While a few molecules that formally incorporate two Blatter radicals have been investigated, they possess singlet (S = 0) ground states and can be classified as zwitterions (tetraphenylhexaazaanthracene = TPHA) or singlet diradicaloids.[26,27] Nevertheless, the 1,2,4-benzotriazinyl framework provides alternative sites for functionalization to facilitate design of novel high-spin systems.

We envisaged high-spin diradicals based on the Blatter radical substituted with nitronyl nitroxide (**1**) and imino nitroxide (**2**) (Figure 1). Diradicals **1** and **2** take advantage of spin density that

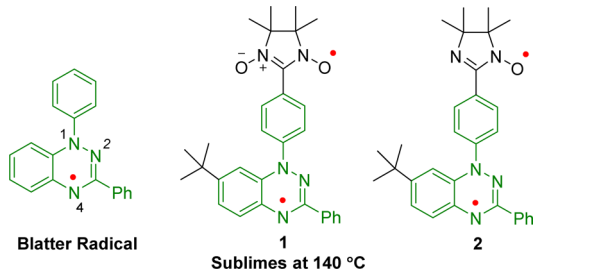

Figure 1. Diradicals **1** and **2** incorporating the Blatter radical.

delocalizes to the N1 phenyl of the 1,2,4-benzotriazinyl radical. This induces ferromagnetic interactions through the trimethylenemethane (TMM)-like ferromagnetic coupling of the nitronyl/imino nitroxides.[13−15] Indeed, broken-symmetry density functional theory (BS-UB3LYP/6-31G(d,p)) calculations[28] estimated ΔE_{ST} as ~1.4 kcal mol^{-1} for **1** and ~0.6 kcal mol^{-1} for **2** (Supporting Information (SI)).[29] Encouraged by the results, we were intrigued to experimentally determine the ΔE_{ST} and the thermal robustness of these diradicals.

Here we report the synthesis and study of high-spin diradicals **1** and **2** (Scheme 1). Diradical **1** is thermally robust, with stability up to ~175 °C under inert atmosphere, and it sublimes under high vacuum at 140 °C with no significant decomposition. Diradical **2**, however, begins to decompose at ~75 °C.

Our synthetic strategy takes advantage of the rather unusual stability of the Blatter radical, such that it can undergo many ordinary chemical transformations.[30] Cyano-substituted Blatter

Received: May 17, 2016
Published: July 19, 2016

DOI: 10.1021/jacs.6b05080
J. Am. Chem. Soc. 2016, 138, 9377−9380

Scheme 1. Synthesis of 1 and 2

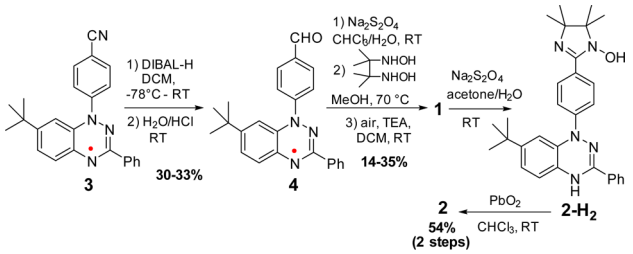

radical **3** was synthesized using procedures similar to those available in the literature.[31−34] Treatment of **3** with DIBAL-H and subsequent hydrolysis of the imine group provides formyl-substituted Blatter radical **4**. Reduction of radical **4** followed by condensation with 2,3-bis(hydroxyamino)-2,3-dimethylbutane[35] and aerobic oxidation provides diradical **1**. The nitronyl nitroxide moiety of **1** can then be converted into the corresponding imino nitroxide moiety of **2** by utilizing a strong reductant (providing **2-H$_2$**) followed by reoxidation with lead(IV) dioxide. The diradicals possess sufficient stability to be purified on silica with no additional precautions.

The single crystal geometry of diradical **1** is shown in Figure 2. Notably, the phenyl at the N1 position is twisted relative to both

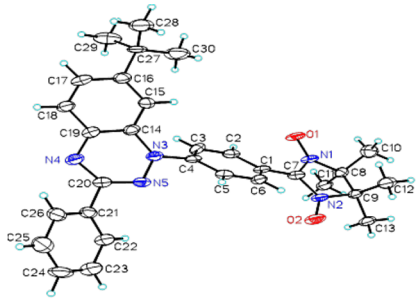

Figure 2. Single-crystal X-ray geometry of **1** with thermal ellipsoids shown at the 50% probability level. Additional details can be found in the SI, Figures S1−S4 and Tables S1 and S2, and CIF file.

the 1,2,4-benzotriazinyl and nitronyl nitroxide moieties (dihedral angles of ∼49° and 30°, respectively). Additional details as well as molecular packing along the different crystallographic axes can be found in the SI.

The structures of diradicals **1** and **2** are also supported by ^{1}H NMR spectra (Figure 3), in which **2-H$_2$** (Scheme 1) serves as a diamagnetic reference. Peak assignments for diradicals **1** and **2** are aided by the plots of DFT-predicted hyperfine coupling constants (hfcc's) vs chemical shift difference ($\Delta\delta$, paramagnetic shift), which are fairly linear for both diradicals (R^2 of 0.9915 and 0.9709 for **1** and **2**, respectively). The prediction of the *tert*-butyl proton hfcc's is complicated by multiple conformations, so this assignment is instead based on peak integration. The majority of remaining protons are predicted to possess hfcc's >0.5 G. Protons for which the ^{1}H hfcc's exceed ∼0.5 G are difficult to observe by ^{1}H NMR at concentrations of ∼1 M due to excessive peak broadening.[18a,36,37] For additional details, as well as hfcc/$\Delta\delta$ plots, see the SI.

Electron paramagnetic resonance (EPR) spectra of 0.4−1.3 mM diradicals **1** and **2** in frozen glasses at low temperatures (Figure 4) can be well-simulated as triplet species. In the case of **2**, monoradical is included in the simulation to account for the less intense center peaks.

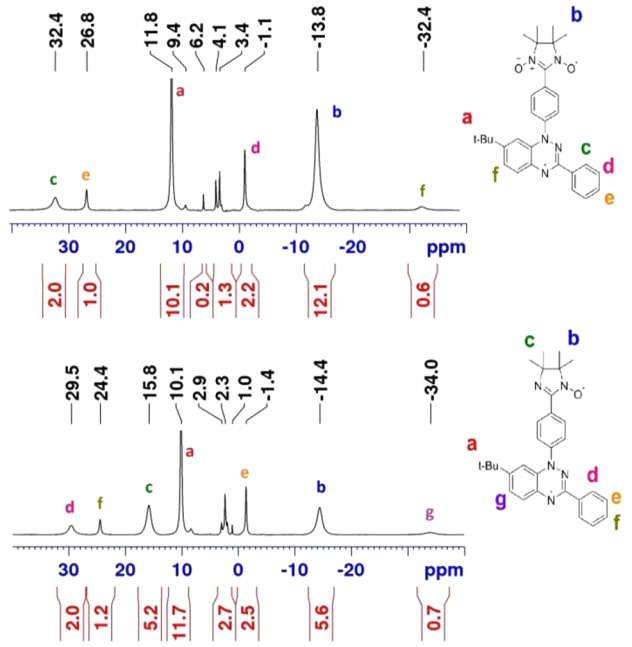

Figure 3. ^{1}H NMR (700 MHz) spectra of 1.6−1.7 M diradical **1** (top) and **2** (bottom) in $CDCl_3$. Additional details can be found in the SI, Figures S17−S19 and Tables S9 and S10.

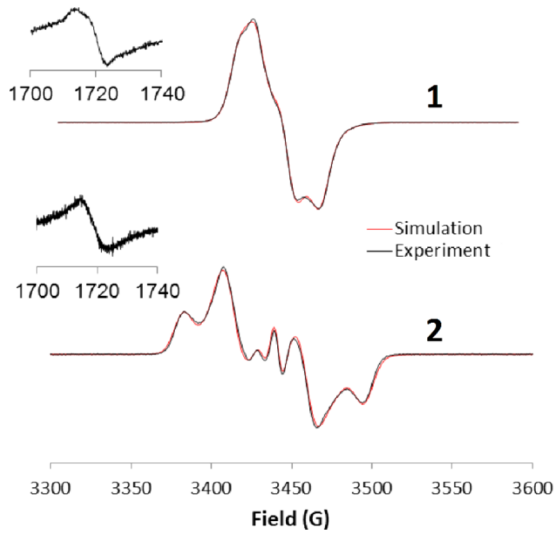

Figure 4. Low-temperature (T = 139−147 K) EPR (X-band, ν = 9.65 GHz) spectra of 1.3 mM diradical **1** and 0.4 mM diradical **2** in a frozen glass (toluene/$CHCl_3$, 4:1). The $\Delta m_s = 2$ transitions are shown as insets. Diradical **2** has smaller center peaks, which are simulated as monoradical impurities (spectral parameters estimated from monoradical **4**). Further details are reported in the SI, Figures S5−S7.

The monoradical spectral parameters for the simulation are estimated from monoradical **4** in frozen glass matrices (see SI for all simulation parameters). More importantly, weak Δm_s = 2 transitions are detected for each diradical, as expected for diradicals with relatively low values of zero-field splitting (zfs) parameter $|D/hc|$. Notably, the zfs parameter $|D/hc|$ in diradical **1** is much smaller than that in diradical **2** ($|D/hc| = 2.32 \times 10^{-3}$ and 5.58×10^{-3} cm^{-1} for **1** and **2**, respectively). This trend is predicted to a lesser extent with B3LYP/EPR-II calculations ($D/hc = -5.47 \times 10^{-3}$ and -6.91×10^{-3} cm^{-1} for **1** and **2**, respectively).[38] These methods tend to overestimate components of the **D** tensor for *m*-xylylene-based diradicals.[39−42]

DOI: 10.1021/jacs.6b05080
J. Am. Chem. Soc. 2016, 138, 9377−9380

EPR spectra of both **1** and **2** show unresolved hyperfine coupling. Line broadening along the molecular *y*-axis (second largest axis of the **D** tensor) in both diradicals is assumed to be due to the unresolved hyperfine coupling to five nitrogens (in both diradicals, the line width along the *y* direction is 3−4 times the line width along the *x* or *z* directions). Together with $D/hc < 0$ predicted for both diradicals, this suggests the overall spin density possesses a "prolate-like" shape in contrast to planar aminyl diradicals.[39]

To determine the triplet ground state and ΔE_{ST} for **1**, we measure χT, the product of paramagnetic susceptibility (χ) and temperature (T), in the $T = 111-320$ K range using quantitative EPR spectroscopy.

We measure values of χT for **1** in toluene/chloroform (4:1) or in dibutyl phthalate (DBP) using a spin-counting standard (eq 1).

$$\chi T = \{[\mathrm{std}]/[\mathbf{1}]\} \times \{\mathrm{Int}_{\mathbf{1}}/\mathrm{Int}_{\mathrm{std}}\}\{(\times 1/2) \times S(S+1)_{\mathrm{std}}\} \quad (1)$$

Each data point in Figure 5 corresponds to multiple independent measurements of χT, i.e., 4−8 independent measurements of **1** and the same number of independent measurements of a nitroxide (TEMPONE) standard. Generally, the data points at higher temperatures required more measurements to obtain a reasonable value of standard error (SE). To ensure that multiple measurements of χT are independent, diradical **1** and TEMPONE (dissolved in the same solvent) were measured in an alternating sequence so that each sample was warmed (or cooled) to room temperature in between successive measurements.[40,41] Although the data obtained by this technique exhibits more scatter relative to SQUID magnetometry,[19,39,43] the EPR-based method is advantageous for stable diradicals. This method permits evaluation of χT in both rigid matrices and in fluid solution at higher temperatures (up to 320 K), while SQUID measurements are typically limited to rigid matrices.

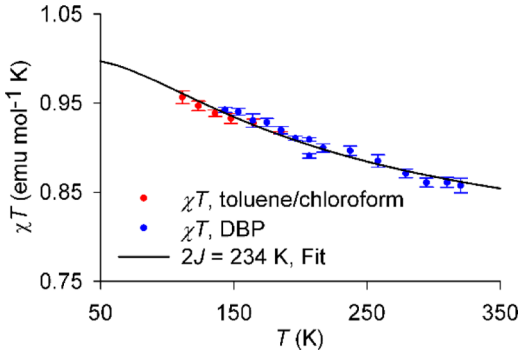

Figure 5. Quantitative EPR spectroscopy of diradical **1**: experimental values of χT (mean ± SE), the product of paramagnetic susceptibility (χ) and T in the $T = 111-320$ K range and numerical one-parameter fit with the variable parameter, $2J/k_B = 234 \pm 36$ K (mean ± SE), and with weight of $1/\chi$. Further details are reported in the SI, Tables S3−S5 and Figure S8.

The highly robust stability of diradical **1** facilitates sublimation under high vacuum ($p \approx 6 \times 10^{-6}$ mbar) at temperatures as high as 140 °C with no significant decomposition. Our thermogravimetric analysis/differential scanning calorimetry results suggest that thermal decomposition of **1** begins at ~175 °C (Figure 6). Indeed, annealing **1** at 200 °C under N_2 for 15 min leads to complete decomposition of the nitronyl nitroxide radical, while the Blatter radical remains largely intact (as evidenced by EPR). On the other hand, diradical **2** begins to decompose at ~75 °C (SI, Figures S12−S16).

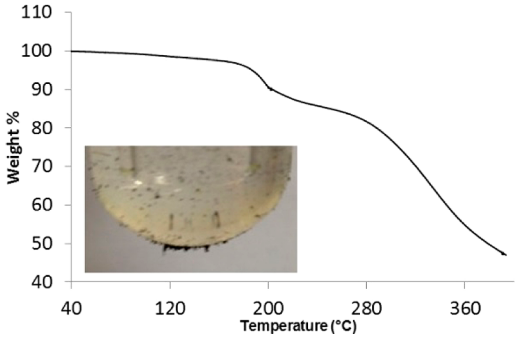

Figure 6. Thermogravimetric analysis (TGA) of diradical **1** under N_2; heating rate = 5 °C min^{-1}. Inset: Diradical **1** after sublimation at $T = 140$ °C, $p \approx 6 \times 10^{-6}$ mbar. We carried out additional experiments to confirm the purity of **1** following sublimation, as well as confirm that the TGA weight loss from 175 to 200 °C corresponds to decomposition of the nitronyl nitroxide moiety (see SI, Figures S12−S16).

Is it possible to augment ΔE_{ST} and still maintain this extraordinary stability? Our more recent DFT calculations suggest that by altering the connectivity of the same radical units (for instance, in diradical **5**, Figure 7), it should be possible to increase the magnitude of ΔE_{ST} by a factor of 2−2.5.[29] Given that BS-DFT overestimates ΔE_{ST} for **1**,[29] an actual $\Delta E_{ST} = 1-2$ kcal mol^{-1} is likely for putative diradical **5**. Using a Boltzmann distribution,[2] such a singlet−triplet gap would lead to 95−99% occupancy of the triplet ground state at room temperature.

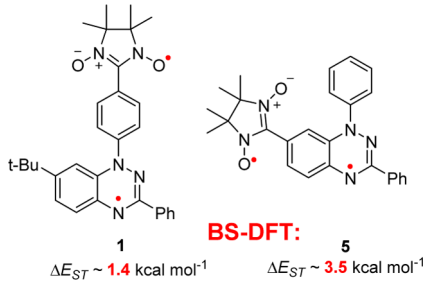

Figure 7. BS-DFT (UB3LYP/6-31G(d,p)) estimates of ΔE_{ST} for diradical **1** and putative diradical **5**. For additional details, see the SI, Tables S7 and S8.

Thus, we anticipate it will be possible to obtain high-spin diradicals with very robust high-temperature stability and full or near-full occupation of the triplet ground state at ambient temperatures. Current efforts are underway in the syntheses of similar diradicals with increased ΔE_{ST} (e.g., **5**), as well as the planned investigation of thin-film properties of **1** for future applications in spintronics.

■ ASSOCIATED CONTENT

Supporting Information

The Supporting Information is available free of charge on the ACS Publications website at DOI: 10.1021/jacs.6b05080.

General procedures and materials, additional experimental details, and complete ref 28 (PDF)

X-ray crystallographic files for **1** (CIF)

■ AUTHOR INFORMATION

Corresponding Author

*arajca1@unl.edu

DOI: 10.1021/jacs.6b05080
J. Am. Chem. Soc. 2016, 138, 9377−9380

Notes

The authors declare no competing financial interest.

■ ACKNOWLEDGMENTS

We thank the NSF Chemistry Division for support of this research under Grant No. CHE-1362454.

■ REFERENCES

(1) Rajca, A. *Chem. Rev.* **1994**, *94*, 871−893.
(2) Gallagher, N. M.; Olankitwanit, A.; Rajca, A. *J. Org. Chem.* **2015**, *80*, 1291−1298.
(3) Ratera, L.; Veciana, J. *Chem. Soc. Rev.* **2012**, *41*, 303−349.
(4) Abe, M. *Chem. Rev.* **2013**, *113*, 7011−7088.
(5) Rajca, A.; Wongsriratanakul, J.; Rajca, S. *Science* **2001**, *294*, 1503−1505.
(6) Rajca, A. *Adv. Phys. Org. Chem.* **2005**, *40*, 153−159.
(7) Wingate, A. J.; Boudouris, B. W. *J. Polym. Sci., Part A: Polym. Chem.* **2016**, *54*, 1875−1894.
(8) Sanvito, S. *Chem. Soc. Rev.* **2011**, *40*, 3336−3355.
(9) Shil, S.; Bhattacharya, D.; Misra, A.; Klein, D. J. *Phys. Chem. Chem. Phys.* **2015**, *17*, 23378−23383.
(10) Tsuji, Y.; Hoffmann, R.; Strange, M.; Solomon, G. C. *Proc. Natl. Acad. Sci. U. S. A.* **2016**, *113*, E413−E419.
(11) Gaudenzi, R.; Burzuri, E.; Reta, D.; Moreira, I. de P. R.; Bromley, S. T.; Rovira, C.; Veciana, J.; van der Zant, H. S. J. *Nano Lett.* **2016**, *16*, 2066−2071.
(12) Herrmann, C.; Solomon, G. C.; Ratner, M. A. *J. Am. Chem. Soc.* **2010**, *132*, 3682−3684.
(13) Jahn, B. O.; Ottosson, H.; Galperin, M.; Fransson, J. *ACS Nano* **2013**, *7*, 1064−1071.
(14) Hiraoka, S.; Okamoto, T.; Kozaki, M.; Shiomi, D.; Sato, K.; Takui, T.; Okada, K. *J. Am. Chem. Soc.* **2004**, *126*, 58−59.
(15) Suzuki, S.; Furui, T.; Kuratsu, M.; Kozaki, M.; Shiomi, D.; Sato, K.; Takui, T.; Okada, K. *J. Am. Chem. Soc.* **2010**, *132*, 15908−15910.
(16) Inoue, K.; Iwamura, H. *Angew. Chem., Int. Ed. Engl.* **1995**, *34*, 927−928.
(17) Rajca, A.; Shiraishi, K.; Rajca, S. *Chem. Commun.* **2009**, 4372−4374.
(18) (a) Rajca, A.; Takahashi, M.; Pink, M.; Spagnol, G.; Rajca, S. *J. Am. Chem. Soc.* **2007**, *129*, 10159−10170. (b) Rassat, A.; Sieveking, U. *Angew. Chem., Int. Ed. Engl.* **1972**, *11*, 303−304.
(19) Boratynski, P. J.; Pink, M.; Rajca, S.; Rajca, A. *Angew. Chem., Int. Ed.* **2010**, *49*, 5459−5462.
(20) Shultz, D. A.; Fico, R. M.; Lee, H.; Kampf, J. W.; Kirschbaum, K.; Pinkerton, A. A.; Boyle, P. D. *J. Am. Chem. Soc.* **2003**, *125*, 15426−15432.
(21) Fukuzaki, E.; Nishide, H. *J. Am. Chem. Soc.* **2006**, *128*, 996−1001.
(22) (a) Veciana, J.; Rovira, C.; Crespo, M. I.; Armet, O.; Domingo, V. M.; Palacio, F. *J. Am. Chem. Soc.* **1991**, *113*, 2552−2561. (b) Rajca, A.; Utamapanya, S. *J. Org. Chem.* **1992**, *57*, 1760−1767.
(23) Forrest, S. R. *Chem. Rev.* **1997**, *97*, 1793−1896.
(24) Ciccullo, F.; Gallagher, N. M.; Geladari, O.; Chasse, T.; Rajca, A.; Casu, M. B. *ACS Appl. Mater. Interfaces* **2016**, *8*, 1805−1812.
(25) Constantinides, C. P.; Koutentis, P. A.; Krassos, H.; Rawson, J. M.; Tasiopoulos, A. J. *J. Org. Chem.* **2011**, *76*, 2798−2806.
(26) (a) Hutchison, K.; Srdanov, G.; Hicks, R.; Yu, H.; Wudl, F.; et al. *J. Am. Chem. Soc.* **1998**, *120*, 2989−2990. (b) Constantinides, C. P.; Zissimou, G. A.; Berezin, A. A.; Ioannou, T. A.; Manoli, M.; Tsokkou, D.; Theodorou, E.; Hayes, S. C.; Koutentis, P. A. *Org. Lett.* **2015**, *17*, 4026−4029.
(27) Zheng, Y.; Miao, M.; Dantelle, G.; Eisenmenger, N. D.; Wu, G.; Yavuz, I.; Chabinyc, M. L.; Houk, K. N.; Wudl, F. *Adv. Mater.* **2015**, *27*, 1718−1723.
(28) Frisch, M. J.; et al.. *Gaussian 09*, revision A.01; Gaussian, Inc.: Wallingford, CT, 2009.
(29) For diradicals **1**, **2**, and **5**, BS-DFT-computed $\Delta E_{ST} \approx 1.4$, 0.6, and 3.5 kcal mol^{-1} at the UB3LYP/6-31G(d,p) level, respectively. While this level of theory overestimates the ΔE_{ST} for ground-state triplet diradicals, this discrepancy worsens when using the UM06-2X functional (instead of UB3LYP), with the corresponding values of $\Delta E_{ST} \approx 2.1$, 0.7, and 3.7 kcal mol^{-1} (Table S7): Mañeru, D. R.; Pal, A. K.; Moreira, I. P. R.; Datta, S. N.; Illas, F. *J. Chem. Theory Comput.* **2014**, *10*, 335−345.
(30) (a) Bodzioch, A.; Zheng, M.; Kaszyński, P.; Utecht, G. *J. Org. Chem.* **2014**, *79*, 7294−7310. (b) Constantinides, C. P.; Obijalska, E.; Kaszyński, P. P. *Org. Lett.* **2016**, *18*, 916−919.
(31) Constantinides, C. P.; Koutentis, P. A. *Adv. Heterocycl. Chem.* **2016**, *119*, 173−207.
(32) Enders, D.; Breuer, K.; Kallfass, U.; Balensiefer, T. *Synthesis* **2003**, *8*, 1292−1295.
(33) Koutentis, P. A.; Re, D. L. *Synthesis* **2010**, *12*, 2075−2079.
(34) Berezin, A. A.; Zissimou, G. A.; Constantinides, C. P.; Beldjoudi, Y.; Rawson, J. M.; Koutentis, P. A. *J. Org. Chem.* **2014**, *79*, 314−327.
(35) Rajca, A.; Pink, M.; Mukherjee, S.; Rajca, S.; Das, K. *Tetrahedron* **2007**, *63*, 10731−10742.
(36) Pearson, G. R.; Walter, R. I. *J. Am. Chem. Soc.* **1977**, *99*, 5262−5268.
(37) Olankitwanit, A.; Kathirvelu, V.; Rajca, S.; Eaton, G. R.; Eaton, S. S.; Rajca, A. *Chem. Commun.* **2011**, *47*, 6443−6445.
(38) Neese, F. *ORCA—An Ab Initio, Density Functional and Semiempirical Program Package*, version 3.0.1; University of Bonn, Germany, 2008.
(39) Rajca, A.; Olankitwanit, A.; Rajca, S. *J. Am. Chem. Soc.* **2011**, *133*, 4750−4753.
(40) Olankitwanit, A.; Pink, M.; Rajca, S.; Rajca, A. *J. Am. Chem. Soc.* **2014**, *136*, 14277−14288.
(41) Olankitwanit, A.; Rajca, S.; Rajca, A. *J. Org. Chem.* **2015**, *80*, 5035−5044.
(42) Sinnecker, S.; Neese, F. *J. Phys. Chem. A* **2006**, *110*, 12267−12275.
(43) Rajca, A.; Olankitwanit, A.; Wang, Y.; Boratynski, P. J.; Pink, M.; Rajca, S. *J. Am. Chem. Soc.* **2013**, *135*, 18205−18215.

DOI: 10.1021/jacs.6b05080
J. Am. Chem. Soc. 2016, 138, 9377−9380